

# **PUSHING THE LIMITS OF 2-D BOUNDARY ELEMENT EDDY CURRENT CODES -- CONNECTIVITY**

## **SUMMARY**

The serious electromechanical designer is faced with optimizing the shape of a device for a number of conflicting criteria. If the design involves eddy currents with saturable media, a true optimization will take a long time, since it requires a lot of information as input with multiple variable variations. If the analyses must be performed in three dimensions, an inordinate amount of computer time is required even for the simplest of problems. No small advantage is accrued if the problem can be approached in two dimensions. The paper outlines a technique for examining eddy currents induced in complex series wound coils for which the connections must be specified to ensure solution accuracy. A boundary element formulation is adopted in which an arbitrary constant vector potential is assigned to each conductor. The connection of the coils can be specified by placing additional constraints on these vector potentials. The technique is tested against two experiments involving forces imposed on flux eliminating coils.

### **Integrated Engineering Software - Website Links**

[Home](#)

[Products](#)

[Support](#)

[Technical Papers](#)

*"Page Down" or use scroll bars to read the article*



## **PUSHING THE LIMITS OF 2-D BOUNDARY ELEMENT EDDY CURRENT CODES -- CONNECTIVITY**

DALIAN ZHENG

*Integrated Engineering Software, #46-1313 Border Place, Winnipeg, Manitoba, Canada*

KENT R. DAVEY

*American MAGLEV, Inc., P.O. Box 10, Edgewater, FL 32132, U.S.A.*

RAY ZOWARKA AND SID PRATAP

*Center for Electromechanics, UT-Austin, Pickle Research Campus Bldg. 133, MC R7000, Austin, TX 78712, U.S.A.*

### **SUMMARY**

The serious electromechanical designer is faced with optimizing the shape of a device for a number of conflicting criteria. If the design involves eddy currents with saturable media, a true optimization will take a long time, since it requires a lot of information as input with multiple variable variations. If the analyses must be performed in three dimensions, an inordinate amount of computer time is required even for the simplest of problems. No small advantage is accrued if the problem can be approached in two dimensions. The paper outlines a technique for examining eddy currents induced in complex series wound coils for which the connections must be specified to ensure solution accuracy. A boundary element formulation is adopted in which an arbitrary constant vector potential is assigned to each conductor. The connection of the coils can be specified by placing additional constraints on these vector potentials. The technique is tested against two experiments involving forces imposed on flux eliminating coils.

### **INTRODUCTION**

Although three-dimensional eddy current codes have received much attention over the past two years,<sup>1,2</sup> their usefulness in optimizing a design is limited due to the long execution time. Design optimizations such as that suggested by Reference 3 require a lot of information to run an efficient inverse calculation. Geometries involving series wound coils virtually demand a three-dimensional analysis unless an efficient means of defining the connection of the coils can be realized. This paper outlines a boundary element method (BEM) which allows the connection of isolated coils to be defined.

One area in which the use of such coils is important is in high speed MAGnetically LEVitated (MAGLEV) vehicles. Here flux eliminating coils such as the null flux coil are used to produce the lift on the vehicle by induction.<sup>4</sup> We seek to apply this technique in the force prediction eliminating coils.

## THEORY

The goal of a boundary element formulation is encapsulated in Figure 1. Each conducting object is to be replaced with a double layer skin of surface current. The fictitious layer of surface current on the outer layer of the body will serve to reflect the body's induced field signature exterior to the body. The layer of surface current just interior to the body is responsible for the complete field interior to the body. These surface currents are chosen to guarantee that the tangential  $H$  field is continuous,  $\hat{n} \times \|\vec{H}\| = 0$  and the normal  $B$  field is continuous  $\hat{n} \cdot \|\vec{B}\| = 0$ . We follow the leads found in References 5 and 6 for this development. Combining Ampers's and Faraday's laws yields the relation

$$\nabla_x \nabla_x \vec{A} - k^2 \vec{A} = \mu \vec{J}^i - j\omega \epsilon' \mu \nabla \Phi \tag{1}$$

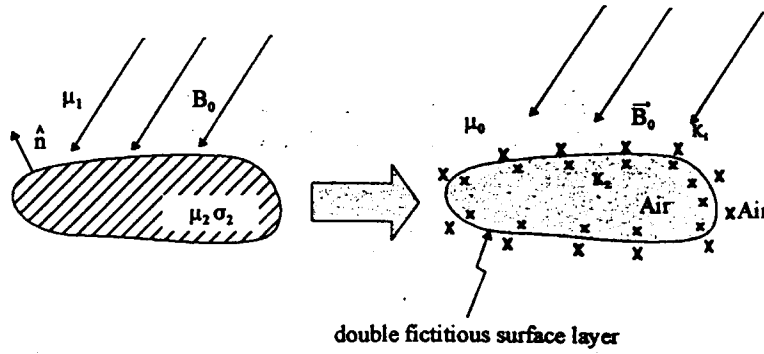


Figure 1. Geometry for double layer boundary element formulation

where  $\epsilon' = \epsilon - j \frac{\sigma}{\omega}$ ,  $k^2 = \omega^2 \epsilon' \mu$ ,  $\vec{E} = -j\omega \vec{A} - \nabla \Phi$  and  $\vec{J}^i$  represents external imposed current density. By adopting the Lorentz gauge

$$\nabla \cdot \vec{A} = -j\omega \epsilon' \mu \phi \tag{2}$$

(1) reduces to

$$\nabla^2 \vec{A} + k^2 \vec{A} = -\mu \vec{J}^i \tag{3}$$

The solution of the vector Helmholtz equation (3) at some field point  $r$  due to a source point  $r'$  is

$$\vec{A}(\vec{r}) = \mu \int_v G(\vec{r}, \vec{r}') \vec{J}^i(\vec{r}') dV \tag{4}$$

In two-dimensional space, Green's function involves the zero-order Hankel function of the second kind and  $R \equiv |\vec{r} - \vec{r}'|$ , as

$$G(\vec{r}, \vec{r}') = \frac{1}{4j} H_0^{(2)}(kR) \quad (5)$$

Now it remains to impose the boundary conditions. Based on the gauge condition (2), both the electric field and the magnetic field intensity can be expressed in terms of the vector potential as

$$\vec{E} = -j\omega\vec{A} - \frac{j}{\omega\epsilon'\mu} \nabla\nabla \cdot \vec{A} \quad (6)$$

$$\vec{H} = \frac{1}{\mu} \nabla \times \vec{A} \quad (7)$$

In two dimensions, it necessarily follows that  $\nabla \cdot \vec{A} = 0$  since  $\vec{A}$  has only one component, and thus

$$\vec{E} = -j\omega\vec{A} \quad (8)$$

Thus in two dimensions, enforcing  $\hat{n} \cdot \vec{B} = 0$  is synonymous with enforcing  $\hat{n} \times \vec{E} = 0$ .

The electric or magnetic field in the interior region of the body is that due to the fictitious surface current  $K_2$ , while the field in the exterior of the region is that resulting from the surface current  $K_1$  plus all impressed sources. Another way of representing the boundary conditions on the interface  $S$  with an outward normal  $\hat{n}$  in terms of the components of  $E$  and  $H$  is:

$$\hat{n}x[\vec{E}_1^+(\vec{r}; \vec{K}_1) - \vec{E}_2^-(\vec{r}; K_2)] = -\hat{n}x\vec{E}^i(\vec{r}), \quad \vec{r} \in S \quad (9)$$

$$\hat{n}x[\vec{H}_1^+(\vec{r}; K_1) - \vec{H}_2^-(\vec{r}; K_2)] = -\hat{n}x\vec{H}^i(\vec{r}), \quad r \in S \quad (10)$$

For the work in this paper there is no imposed  $E$  field, but we keep it for completeness. Combining (9) and (10) with (4) yields the final result

$$j\omega \left[ \mu_1 \int_s G(k_1; \vec{r}, \vec{r}') \vec{K}_1(\vec{r}') dS' - \mu_2 \int_s G(k_2; \vec{r}, \vec{r}') \vec{K}_2(\vec{r}') dS' \right] = -\vec{E}_z^i(\vec{r}), \quad \vec{r} \in S \quad (11)$$

$$-\int_s \frac{\partial G(k_1; \vec{r}, \vec{r}')}{\partial n} \vec{K}_1(\vec{r}') dS' + \mu_2 \int_s \frac{\partial G(k_2; \vec{r}, \vec{r}')}{\partial n} \vec{K}_2(\vec{r}') dS' + \frac{\vec{K}_1(\vec{r}) + \vec{K}_2(\vec{r})}{2} = -\hat{n} x \vec{H}^i(\vec{r}), \quad \vec{r} \in S \quad (12)$$

The surfaces are discretized into elements; the unknowns are assumed linear over each element and the Galerkin technique used to build a matrix for determining the unknowns.

### SPECIFYING CONNECTIVITY

The connection of conductors is specified as follows. An additional constant vector potential  $A_c$  is assumed within the interior of each conductor so that (4) on the interior of a region (e.g. region 2) becomes

$$\vec{A}(\vec{r}) = \mu_2 \int_v G(\vec{r}, \vec{r}') \vec{K}_2(\vec{r}') dV' + \vec{A}_{c2} \quad (13)$$

An additional unknown constant vector potential is assigned to the interior of every region for which a connection condition is to be specified. For purposes of discussion there are four separate regions which are part of the same conductor. Assume the current is in the same direction for conductors 1 and 3 and likewise for conductors 2 and 4. The above assignment would imply the need to generate four additional equations. Three of these four equations come from the requirement that each region carry the same induced current, i.e.

$$\oint_{s_1^+} \vec{H} \cdot \vec{dl} = -\oint_{s_2^+} \vec{H} \cdot \vec{dl} \quad (14)$$

$$\oint_{s_2^+} \vec{H} \cdot \vec{dl} = -\oint_{s_3^+} \vec{H} \cdot \vec{dl} \quad (15)$$

$$\oint_{s_3^+} \vec{H} \cdot \vec{dl} = -\oint_{s_4^+} \vec{H} \cdot \vec{dl} \quad (16)$$

The final equation recognizes that the four windings which constitute the series wound coil do not have a separate potential imposed across them; the current which flows is that due to magnetic induction by a changing magnetic field. There is no imposed  $-\nabla\Phi$ . Thus, the final condition to be imposed is

$$\vec{A}_{c1} - \vec{A}_{c2} + \vec{A}_{c3} - \vec{A}_{c4} = 0 \quad (17)$$

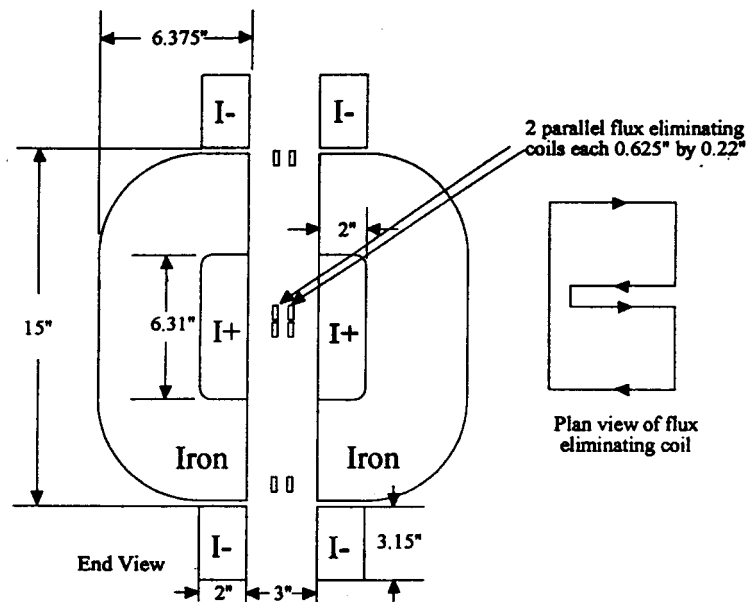


Figure 2. Magnetic yoke surrounding a flux eliminating coil

This condition ensures that the imposed potential (not induced) potential around the loop comprised by the four conductor regions is identically zero. Such a condition forces the current to seek a median value from that witnessed when no such external conditions are imposed. Observe that

$$\oint \vec{E} \cdot d\vec{l} = - \int \frac{d\vec{B}}{dt} \cdot \hat{n} dS + V$$

The surface currents  $\vec{R}$  account for the rate of change of flux. The constant vector potential  $A_c$  is added to account for the imposed electric potential  $V$  which is zero.

## RESULTS

The first problem analysed is the force induced on a flux eliminating coil sandwiched in a magnetizable yoke (Figure 2). The end view for the assembly is depicted in (17). The iron yoke is made of carbon 1010 steel having the  $B/H$  curve shown in Figure 3.

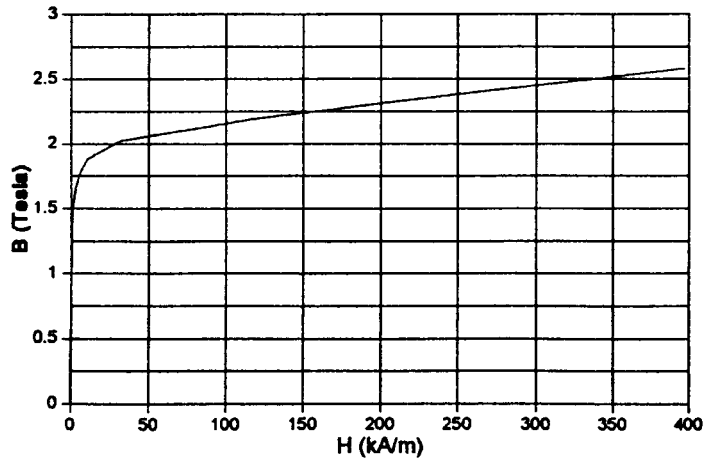


Figure 3. B/H curve for carbon 1010 steel

The average  $B$  field with a 135kA 60 Hz excitation in the airgap is 1.37 T. Two flux eliminating coils in parallel have an inductance of  $187 \mu H$  with a resistance of  $53 m\Omega$ . When the coils are displaced upward vertically 0.25", the flux linking the coil is 0.0059 webers. The equivalent 10-turn coil would therefore have an induced current

$$I_{ind} = \frac{j10(0.0059)377}{j377(187 \times 10^{-6}) + 53 \times 10^{-3}} A \quad (18)$$

The actual length of these coils was 23". The magnet depth was 13". Since there are two vertical lengths of conductor each 13" long contributing to the lift, the lift forces is

$$F = \Re[1.37(10)I_{ind}(26in)(0.0254m/in) \times 4.48lbs/N] = 407lb \quad (19)$$

The 2D lift force predicted was 62.52 lb/in. The equivalent lift must be computed with a 13" magnet using 23" coils. Both the depth of the magnet and the equivalent length of the coil must be adjusted as the overprediction is expected from the failure of the code to estimate the end effects. The following Section addresses a refinement for this problem.

### ROTATING EMBODIMENT

The second problem analyzed was a rotating wheel, the rotor of which contains null flux coils. The null flux coil is simply a series wound "figure 8" shaped coil. The null flux coils rotating between transverse magnets as in Figure 4 yield lift forces on the null flux coil when it is off-centered vertically. Magnets oriented in opposition induced currents to recenter the coils between the magnets. The coils span  $6.75^\circ$  but repeat on  $8^\circ$  centers. The copper coils have a thickness of 0.3125", and are mounted on a 24" radius wheel with the centers of the coils located at a mean radius of 22". Figure 5 shows the layout of the coils between two sets of repulsive magnets and four sets of transverse magnets.

The coils are placed between 1.2" thick magnets with a 0.5" carbon steel back plate as suggested in Figure 6. The iron has a  $B/H$  curve identical to that in Figure 3. The NdFeB magnets have a

coercive force  $H_c=10.4\text{kOe}$  (827.6 kA/m) with a  $B_r=11.2\text{KG}$ (1.12T). The series coil connection is such that it forces current to flow in the same direction in the first and third conductors down, as well as the second and fourth. The coil space area houses a 212-turn winding with a 70% packing factor. As the wheel mounted coils rotate at a speed  $\Omega$ , the coils which span  $\alpha = 6.75^\circ$  see an equivalent electrical frequency  $f$ , based on the tip speed of the wheel  $v$  and the radius  $R$  of

$$f = \frac{1}{2\pi} \frac{180}{\alpha} \frac{v}{R}$$

(20)

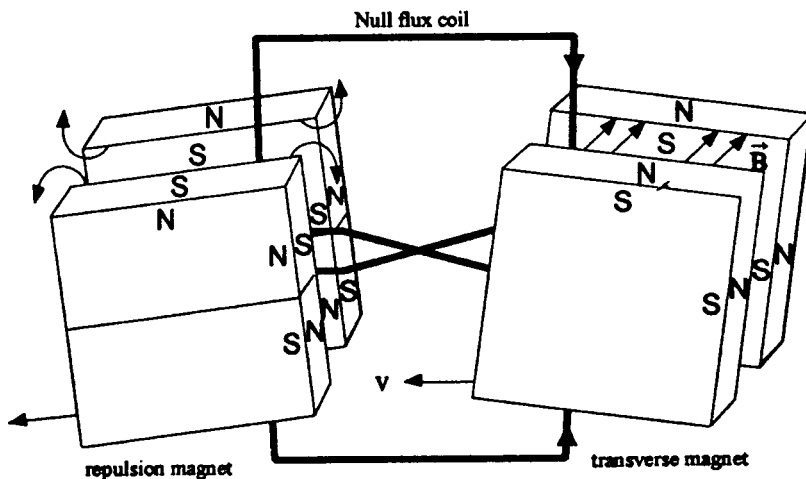


Figure 4. Null flux coils acted upon by transverse magnets and repulsive magnets

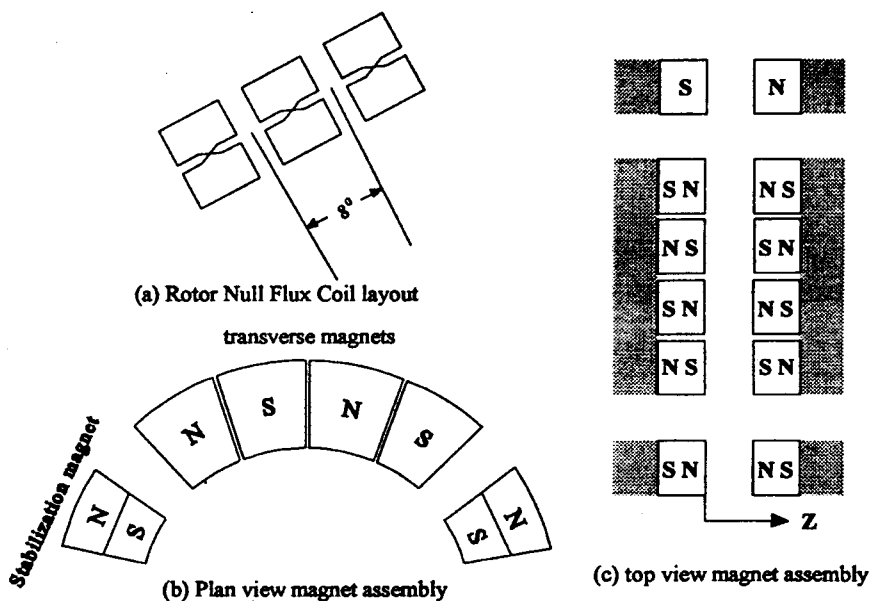


Figure 5. Null flux coil wheel layout



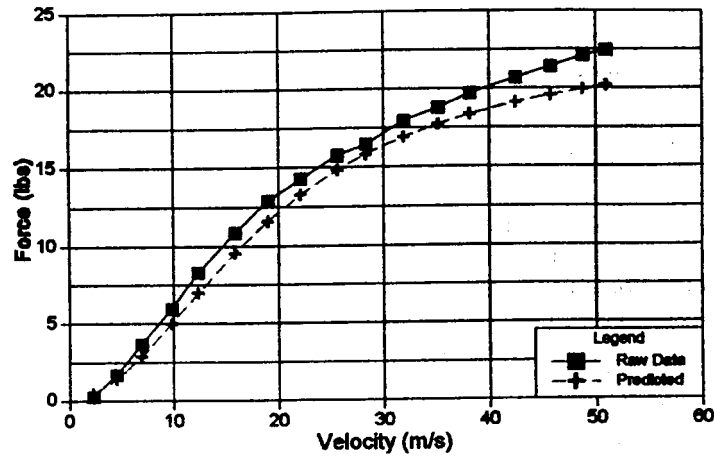


Figure 7. Guidance forces measured against those predicted for null flux test wheel

The upper coil's height is 1.3125" and the depth is 1.875". Applying the correction in (21) to this coil yields a modified conductivity  $\sigma = 2.755\Omega / m$  for the upper coil.

The remaining question remains, "How is the depth accounted for?". A two-dimensional problem computes forces on a per unit depth basis. From Figure 8 it seems appropriate to use the average working straight length of the conductor into the page, i.e.

$$depth = \frac{0.875 + 1.1875}{2} = 1.031" \quad (22)$$

A quantitative way of refining this value if a 3-D program is available is to compute the flux linkage of the magnet with the coil. From 2-D flux linkage, a depth can be computed which yields the same flux linkage when the coil and magnets are aligned. This flux calculation, although 3-D, can be performed statically.

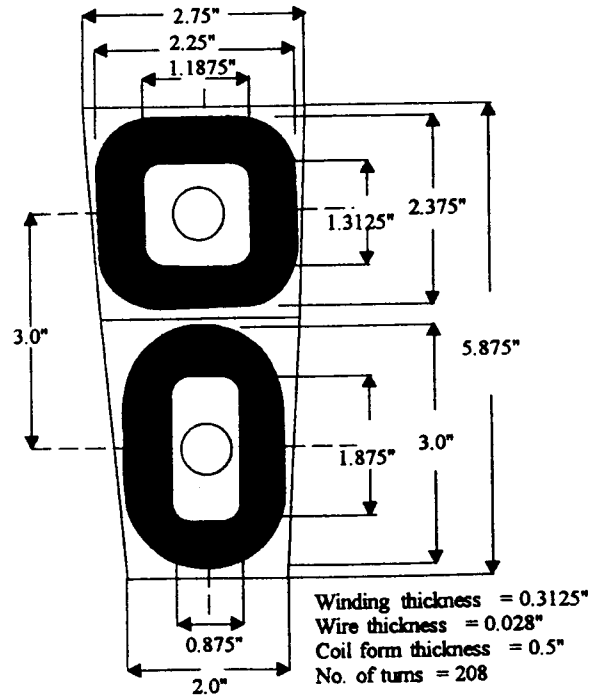


Figure 8. Plan view of the coil layout

## RESULTS

Varying the frequency is equivalent to mapping the guidance force as a function of tip speed. The lateral guidance force was measured against speed using a load cell mounted to the magnet assembly depicted in Figure 5, gimbaling the weight of the magnet assembly. Figure 6 shows a comparison of the forces predicted and measured for the test wheel. Guidance is delivered only when the coil is off-centered laterally; an offset of 0.125" was enforced for this test. The reader acquainted with induction motor torque-speed curves should be aware of the importance of the coil  $L/R$  time constraint's influence on the force-speed curve. Increasing the resistance of the winding flattens the numerical prediction, bringing it more in line with the measured response. A second consideration is that the numerical prediction assumes the coil is in a time-harmonic state. With only a single repulsive magnet on the leading and trailing edge of the assembly, this assumption is not warranted, and thus some error is expected.

The sinusoidal assumption with a series of four transverse magnets in lift is, however, good. The prediction of lift is, however, quite a bit more difficult due to the closure path of the magnetic field into the third dimension. A top view of the transverse magnet assembly is shown in Figure 9. The series of four magnets are drive flux through the 0.5" airgap. This top view is accurate at the average radius for the assembly (20"). In this view, the null flux coil component conductors cannot be represented. One means of dealing with the difficulty of the field closure path is to construct an artificial closure path outside the region of interest is suggested in Figure 10. The surrounding material is arbitrarily selected to have a linear permeability  $\mu_r = 1000$ . The NdFeB magnets are modelled with equivalent surface currents; the strength of these surface currents is chosen to yield the same  $B$  field in the gap as the average field witnessed on the midline of the central magnets of Figure 9. Because the magnets and coils repeat on  $8^\circ$  centers, the expression linking tip velocity to frequency is (20) with  $a = 8^\circ$ . The coil only delivers a lift force when it is off-centered vertically; the variable  $c$  indicating the distance between the top side of the magnets and the top of

the coils was used as this indicator. The two experiments  $c=1.375''$  and  $1.675''$  correspond to a vertical offset of the coils of  $0.48''$  and  $0.73''$ , respectively. The results for  $c = 1.375''$  are shown in Figure 11. The comparable experiment with a larger  $c$  of  $1.675''$  is shown in Figure 12.

## CONCLUSIONS

A technique of dictating coil connectivity is discussed and tested for two distinct problems. The accuracy of the prediction is in keeping with that expected for problems with a relatively small depth. Being able to dictate the connections for the coils affords considerable flexibility in complex optimization designs. The actual shape of the yoke depicted in (17) was selected using multiple parametric analyses to optimize the lift for a MAGLEV vehicle. End effects are accounted for by lowering the conductivity by the ratio of the coil's end turn length to its depth into the page. Fringe effects are accounted for by averaging the working conductor length.

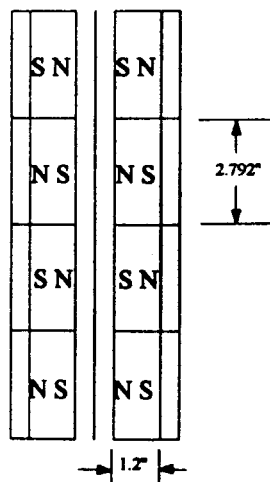


Figure 9. Top view of transverse magnet assembly

## REFERENCES

1. J. Yuan and A. Kost, "A three component boundary element algorithm for three dimensional eddy current calculation", IEEE Trans. Magn., 30, (5), 3028-3031 (1994).
2. T. Morisue and T. Yajima, "The Lorentz gauge vector potential formulation for the boundary integral equation method", IEEE Trans. Magn., 30, (5), 3032-3035 (1995).
3. K. Davey, "Degaussing with BEM and MFS", IEEE Trans. Magn., 30, (5) 3451-3454 (1994).
4. S. Fujiwara and T. Fujimoto, "Characteristics of the combined levitation and guidance TDS MAGLEV system", Trans. Inst. Electr. Eng. Jn., 112-D, (5) 459-466 (1992).
5. Y. Bulent Yildir, K.M. Prasad, and Dalian Zheng, "Computer aided design in electromagnetic systems: Boundary element method and applications", Control Dyn. Syst., 59 167-223 (1993).
6. M.H. Lean, "Dual simple-layer source formulation for two-dimensional eddy current and skin effect problems:", J. Appl. Phys., 57, (1) 3844-3846 (1985).

## **Author's Biographies:**

**Dalian Zheng** received the B.Sc. degree from the Beijing Institute of Aeronautics and Astronautics, China, in 1982, the M.Sc. degree from the Ohio State University, Columbus, in 1985, and the Ph.D. degree from the University of Mississippi, in 1988. From 1988 to 1991 he was a Post-Doctoral Research Associate in the Department of Electrical Engineering at the Texas A&M University in College Station. Currently, he is a research and development engineer at Integrated Engineering Software in Winnipeg, Canada. His major research interests are electromagnetic theory, and numerical methods applied to electromagnetic devices.

**Dr. Kent R. Davey** has been Technical Director of American MAGLEV in Florida since July 1994. Prior to that he was a faculty member at Georgia Institute of Technology in the School of Electrical Engineering. His expertise is in the area of continuum electromechanics and specifically in the computation of electric and magnetic fields and forces using boundary element techniques. He has authored 111 technical papers and reports. He has co-ordinated and directed 1.7 million dollars worth of research in the area of applied electromagnetics, not including the 2 million dollar MAGLEV research effort being undertaken at present.

**Raymond C. Zowarka, Jr.**, was born in San Antonio, TX on 20 March 1950. He received the B.S. degree in engineering science from Trinity University, San Antonio, TX in 1972, and the M.S. degree from The University of Texas at Austin in 1980. He has worked at the Center for Electromechanics at The University of Texas since 1974. As a research scientist at the university he has been actively involved in the Army's electric gun program and continues to perform research on hypervelocity sliding contacts. Currently research interests involve experimental and analytical studies of magnetically levitated trains.

**Saddbarth B. Pratap** was born in Bombay, India, in 1955. He received the Bachelor of Electrical Engineering degree from the University of Bombay in 1979 and the Master of Science in Engineering degree from the University of Texas at Austin in 1982. From 1979 to 1981 he was with the Tata Engineering and Locomotive Company in Pune, India, as an engineer in the Central Plant Engineering Department. Currently he is a Research Associate at the Center for Electromechanics, The University of Texas at Austin (CEM-UT). He has been with CEM-TU since 1982. His research interests include pulsed power systems, electrical machinery and transient electromagnetic diffusion phenomena.

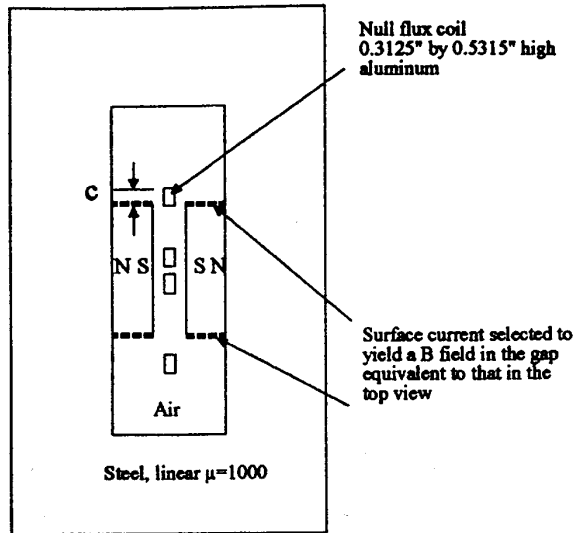


Figure 10. Modified lift assembly to provide an artificial field closure path

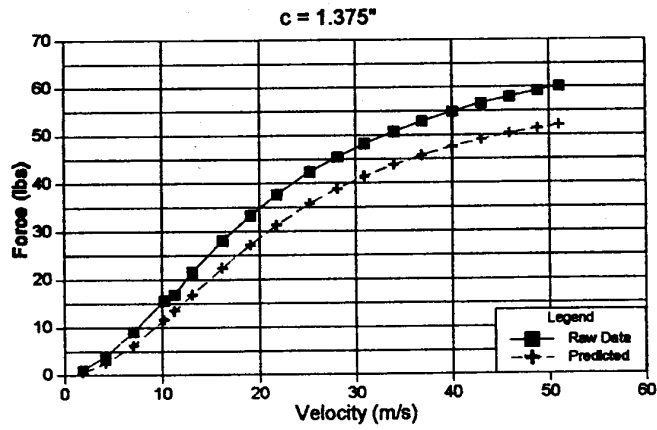


Figure 11. Lift forces from experiment and calculation for  $c = 1.375''$

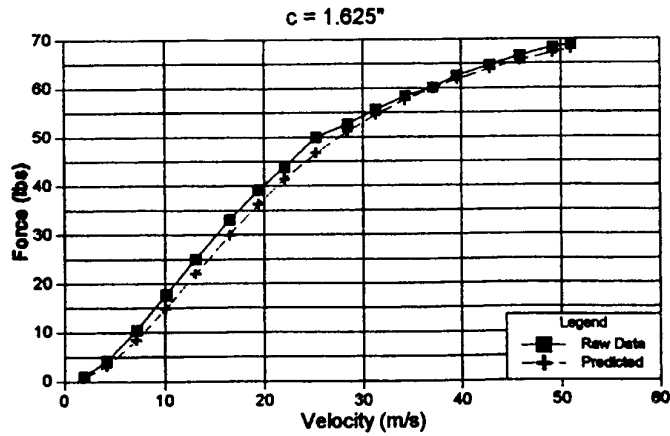


Figure 12. Lift and experimental results for  $c = 1.675''$  displacement